Supporting Information

Copper Inhibition of Triplet-Induced Reactions involving Natural Organic Matter

Yanheng Pan[1], Shikha Garg[2], T. David Waite[2], Xin Yang[1*]

[1] School of Environmental Science and Engineering, Guangdong Provincial Key Laboratory of Environmental Pollution Control and Remediation Technology, Sun Yat-sen University, Guangzhou 510275, China

[2] School of Civil and Environmental Engineering, The University of New South Wales, Sydney, New South Wales 2052, Australia

* Corresponding author, Tel: +86-2039332690, email: yangx36@mail.sysu.edu.cn

22 Pages

16 Figures

2 Tables

Environmental Science & Technology

Supporting Information Contents

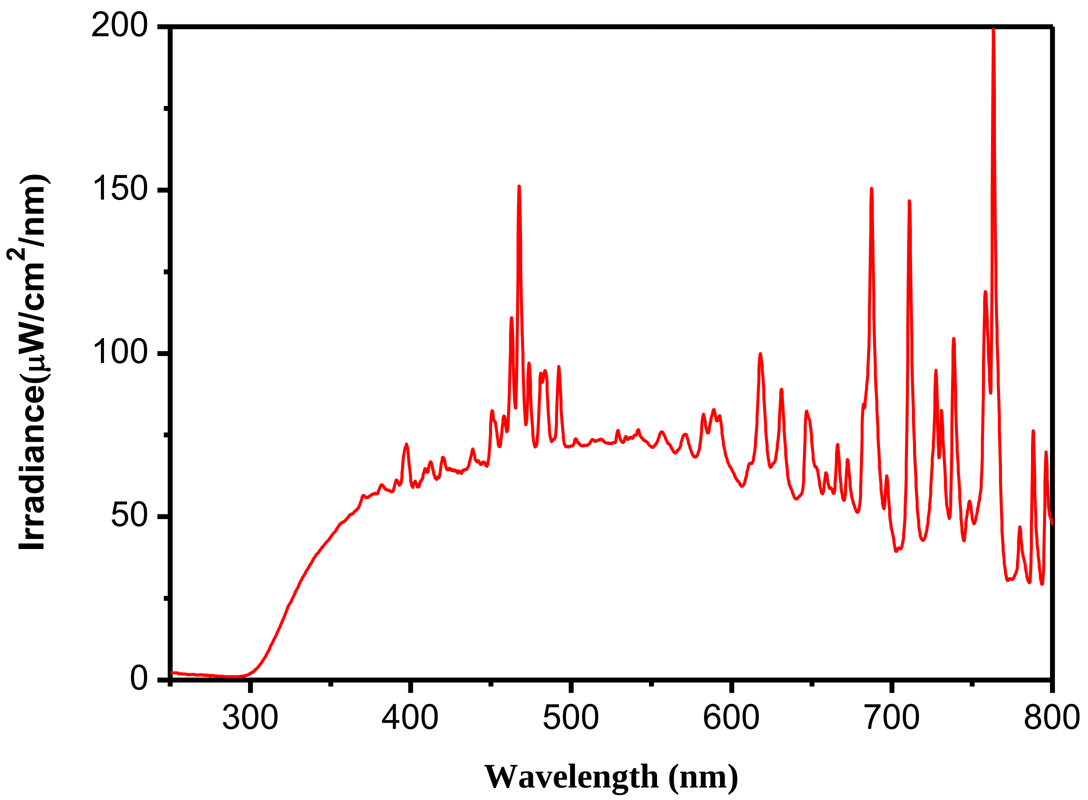

Figure S1. Spectral irradiance from the solar simulator equipped with a Daylight-Q optical filter.

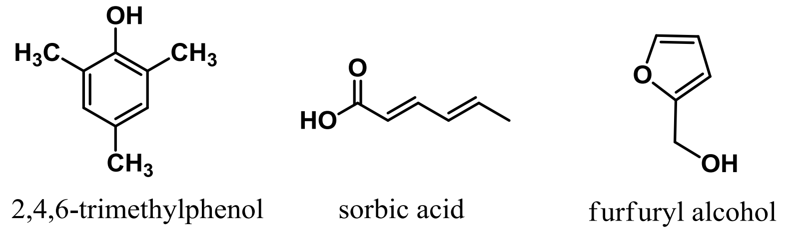

Figure S2. Molecular structures of probe compounds used in this study.

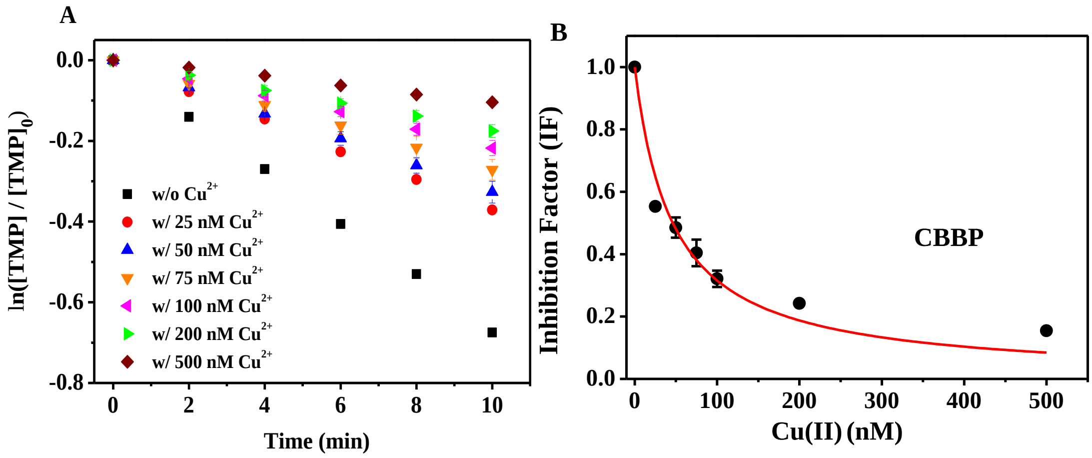

Figure S3. (A) Photosensitized oxidation of 2,4,6-trimethylphenol (TMP, 5 μM) by CBBP in the absence and presence of Cu(II) under simulated sunlight irradiation. (B) Inhibition factor (IF) of Cu(II) for the ^{3}CBBP*-induced oxidation of TMP. Conditions: CBBP = 45 μM, pH = 5.0, DO (dissolved oxygen) = 226 μM.

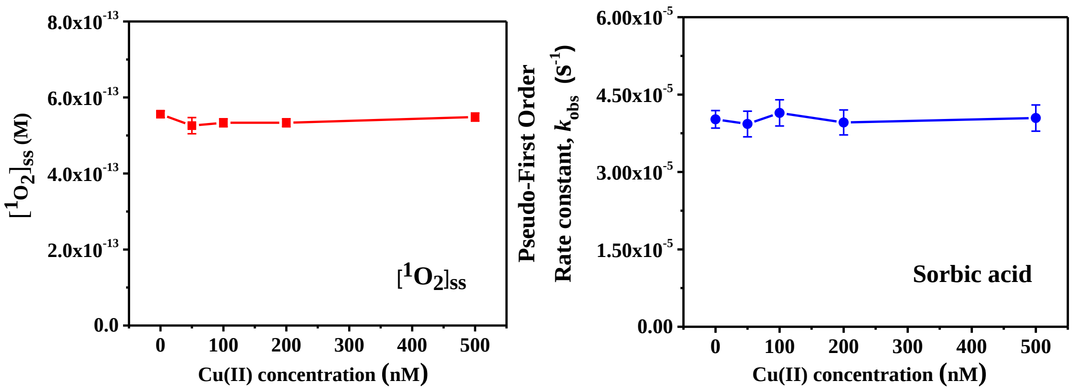

Figure S4. Effect of addition of nanomolar Cu(II) on the steady-state concentrations of $^1O_2$ generated and degradation rate of sorbic acid on photolysis of 10 mg C/L Suwannee River NOM solutions. Conditions: FFA = 30 µM or sorbic acid= 5 µM, pH = 5.0, DO (dissolved oxygen) = 226 µM.

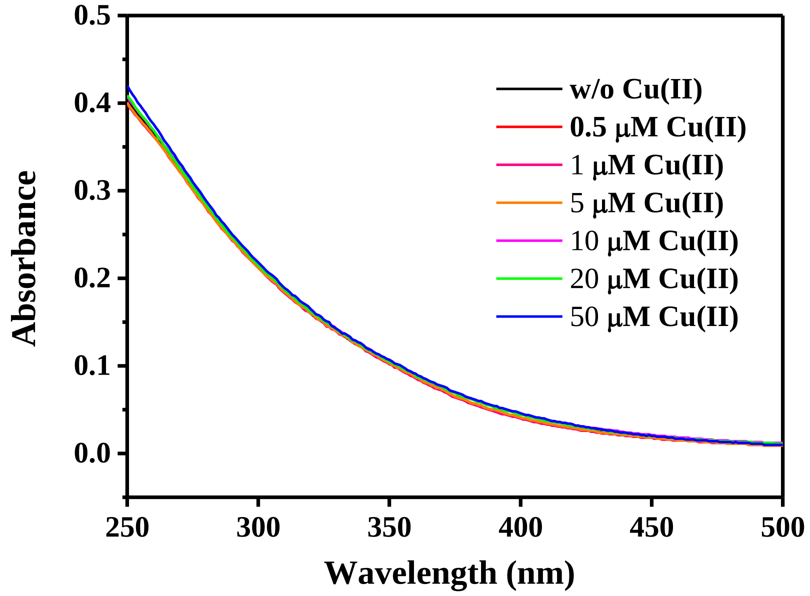

Figure S5. Absorbance spectra for Suwannee River NOM (10 mgC/L) solutions in the absence and presence of Cu(II) at pH =5.0.

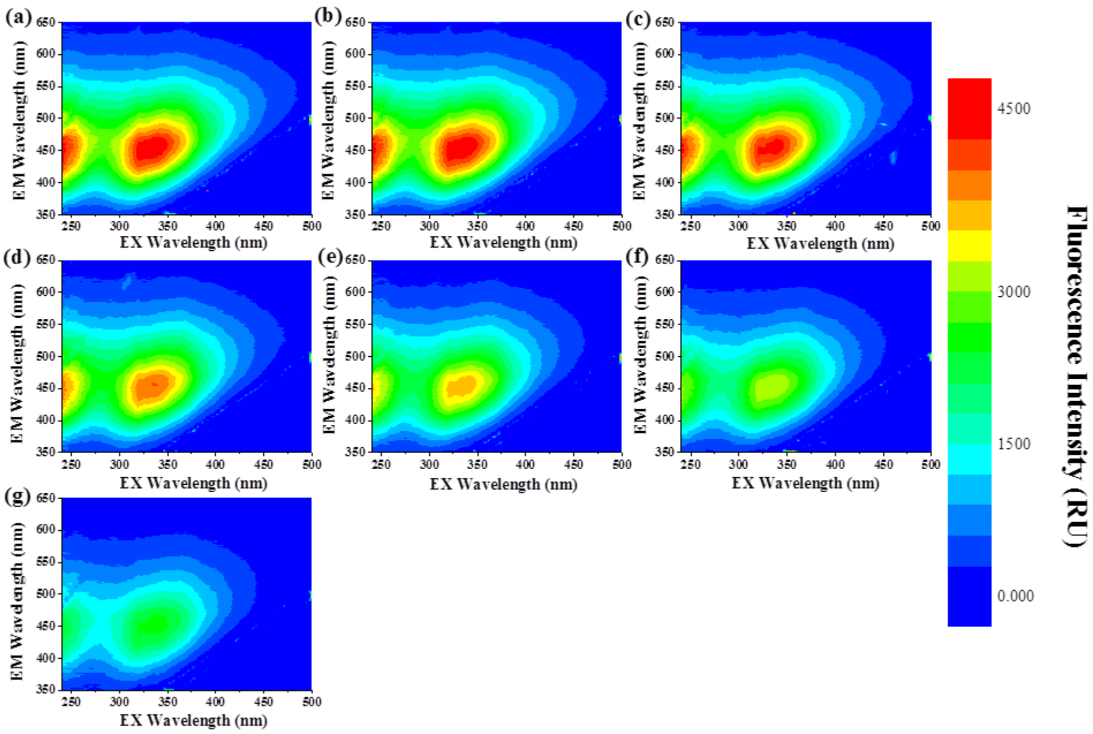

Figure S6. 3D-Fluorescence spectra for Suwannee River NOM (10mg C/L) solutions in the presence of Cu(II) at pH =5.0 (a) 0 nM, (b) 500 nM, (c) 1 µM, (d) 5 µM, (e) 10 µM Cu(II), (f) 20 µM and (g) 50 µM.

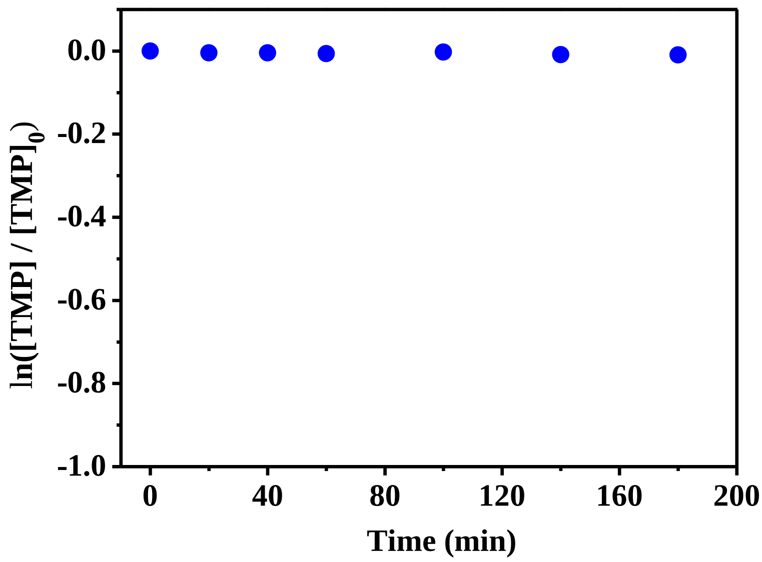

Figure S7. 2,4,6-trimethylphenol (TMP, 5 µM) degradation in non-irradiated 10 mg C/L Suwannee River NOM solutions containing 1 µM Cu(II) at pH =5.0.

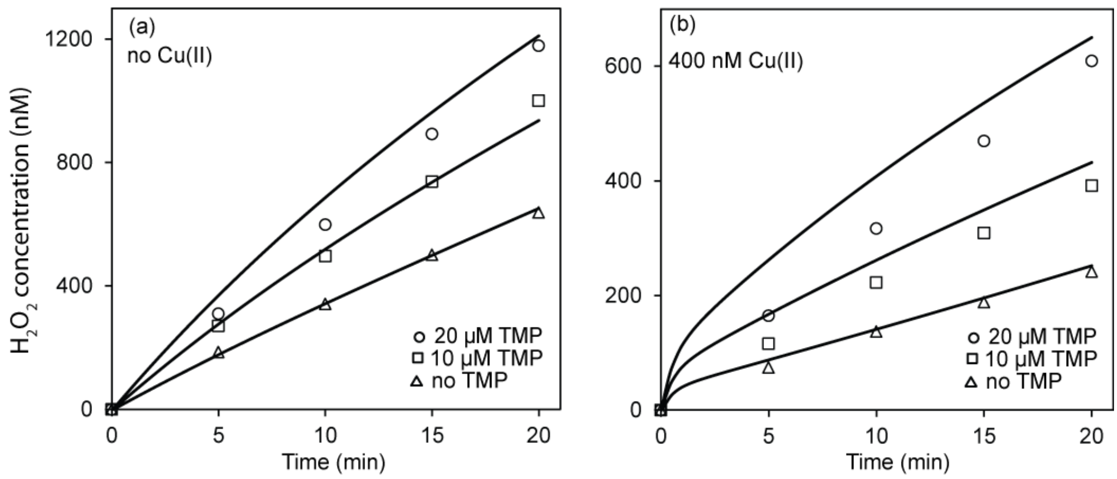

Figure S8. Effect of TMP on H_2O_2 concentration generated on photolysis of 10 mg C/L Suwannee River NOM solutions in the (a) absence and (b) presence of 400 nM Cu(II). Points represent experimentally measured values and lines represent the model predicted concentrations.

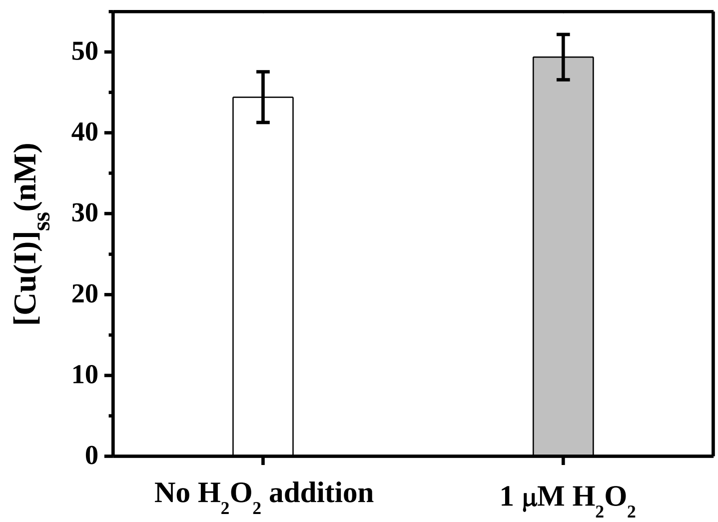

Figure S9. Effect of H_2O_2 addition on the steady-state concentrations of Cu(I) generated under irradiation of Cu(II) in 10 mgC/L SRNOM solution. Conditions: initial Cu(II) concentration = 400 nM, pH = 5.0, DO (dissolved oxygen) = 226 μM.

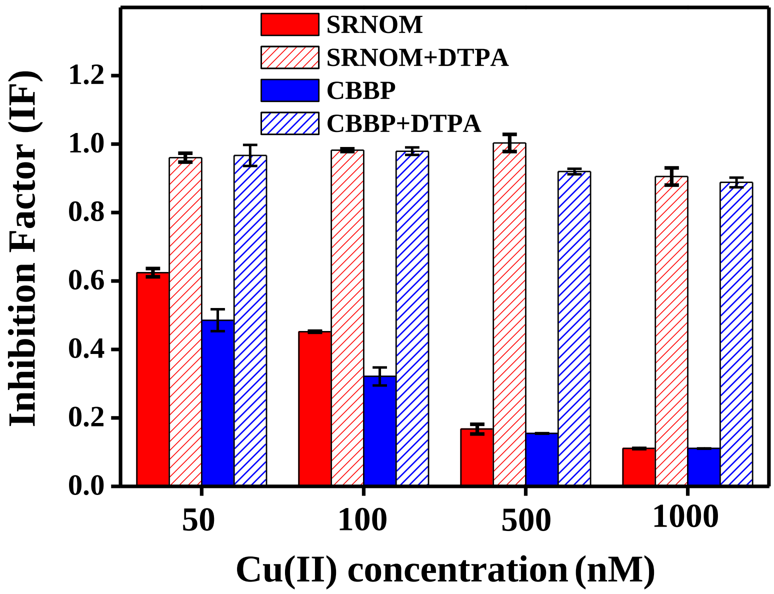

Figure S10. Effect of DTPA addition on the inhibition factor (IF) of Cu(II) for the triplet-induced oxidation of TMP in SRNOM and CBBP systems. Conditions: SRNOM = 10 mg C/L or CBBP = 45 μM, pH = 5.0, DTPA = 5 μM, DO (dissolved oxygen) = 226 μM.

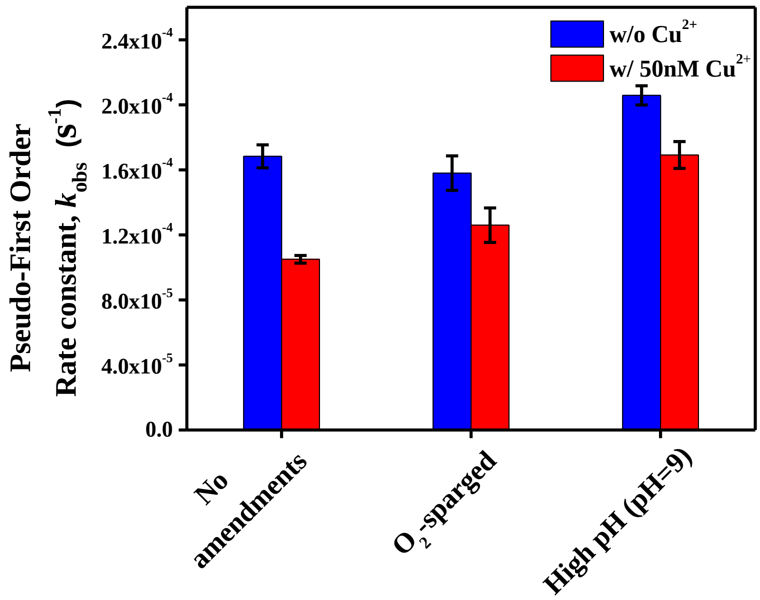

Figure S11. Effect of various treatments on the pseudo-first-order rate constants of TMP (5 μM) in 10 mg C/L SRNOM solutions in the absence and presence of 50 nM Cu(II). No amendments = 10 mg C/L SRNOM at pH = 5.0, DO (dissolved oxygen) = 226 μM. O_2-sparged=10 mg C/L SRNOM at pH = 5.0, DO = 820 μM. High pH= 10 mg C/L SRNOM at pH = 9.0, DO = 226 μM

Text S1. Measurement of high energy ^{3}NOM* probed by sorbate

The formation rates (F_T), loss rate constants (k'_s) and steady-state concentrations ($[^3NOM^*]_{ss}$) of high energy ^{3}NOM* can be calculated from the photosensitized isomerization of sorbic acid (*trans,trans*-hexadienoic acid, *t,t*-HDA). SRNOM solutions containing sorbic acid at five different concentrations (100 μM, 250 μM, 500 μM, 750 μM and 1000 μM) were irradiated for 40 min and was analyzed using HPLC. A Window-Q optical filter was used to cut off light below 315 nm to minimize the self-photoisomerization of *t,t*-HDA. Figure S12 shows the HPLC chromatogram of the irradiated sorbic acid with its four isomers (*c,t*-HDA, *c,c*-HDA, *t,t*-HDA and *t,c*-HDA) in SRNOM solution.

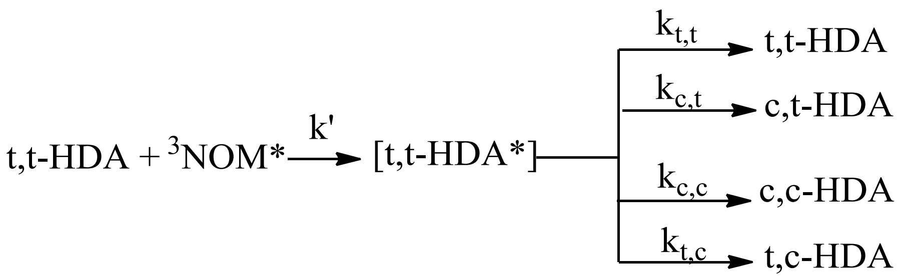

The overall photoisomerization rate of sorbic acid (R_p) was calculated as the sum of *c,t*-HDA, *c,c*-HDA, *t,c*-HDA formation rates and *t,t*-HDA reformation rate subtraction of the minor self-isomerization rate of HDA (S1), which was shown in Figure S13.

$$R_p = R_{c,t\text{-HDA}} + R_{c,c\text{-HDA}} + R_{t,t\text{-HDA}} + R_{t,c\text{-HDA}} - R_{HDA,blank} \quad \text{(S1)}$$

Formation rates of *c,t*-HDA, *c,c*-HDA, and *t,c*-HDA were directly determined while the *t,t*-HDA reformation rate ($R_{t,t\text{-HDA}}$) was calculated based on the measured *t,t*-HDA decay rates and *c,t*-HDA formation rates using the following equation : [1-3]

$$R_{c,t\text{-HDA}} = \frac{d[c,t\text{-HDA}]}{dt} = k_{c,t}[t,t\text{-HDA}^*] \quad \text{(S2)}$$

$$R_{t,t\text{-HDA}} = k_{t,t}[t,t\text{-HDA}^*] = \frac{k_{t,t}}{k_{c,t}}\frac{d[c,t\text{-HDA}]}{dt} \quad \text{(S3)}$$

$$-\frac{d[t,t\text{-HDA}]}{dt} = k_{t,t}[t,t\text{-HDA}^*] - k'[t,t\text{-HDA}] \quad \text{(S4)}$$

Combining S2-S4 one obtained S5

$$-\frac{d[t,t\text{-HDA}]}{dt} = \frac{R_{t,t\text{-HDA}}}{R_{C,t\text{-HDA}}}\frac{d[c,t\text{-HDA}]}{dt} - k'[t,t\text{-HDA}] \quad \text{(S5)}$$

This equation is of the form: $y=c_1x_1+c_2x_2$

The ratio of *t,t*-HDA reformation rate ($R_{t,t\text{-HDA}}$) to *c,t*-HDA formation rate ($R_{t,t\text{-HDA}}$) was derived by a binary linear regression of the equation S5 based on all the sorbate photolysis experiments (n = 20). This value was determined to be 3.14 ±0.14, comparing well to previous results.[1-3]

At steady state, the relationship between the formation rate of ^{3}NOM* (F_T), R_p and the loss rate constant by scavengers (other than *t,t*-HDA) (k'_s) can be linearly expressed as:

$$\frac{[t,t\text{-HDA}]}{R_P} = \frac{[t,t\text{-HDA}]}{F_T} + \frac{k'_S}{F_T k_{t,t\text{-HDA}}} \quad \text{(S6)}$$

where [*t,t*-HDA] is the initial concentration of *t,t*-HDA, $k_{t,t\text{-HDA}}$ is the estimated second-order rate constant (= 6.2×10^8 M^{-1} s^{-1} [4]) for reaction between *t,t*-HDA and triplet states of SRNOM. F_T and k'_s can be calculated from the slope and intercept, respectively, of the above linear fit. Thus, the steady-state triplet concentration, $[^3NOM^*]_{ss}$, can be obtained from S7.

$$\frac{F_T}{k'_S} = [^3NOM^*]_{ss} \tag{S7}$$

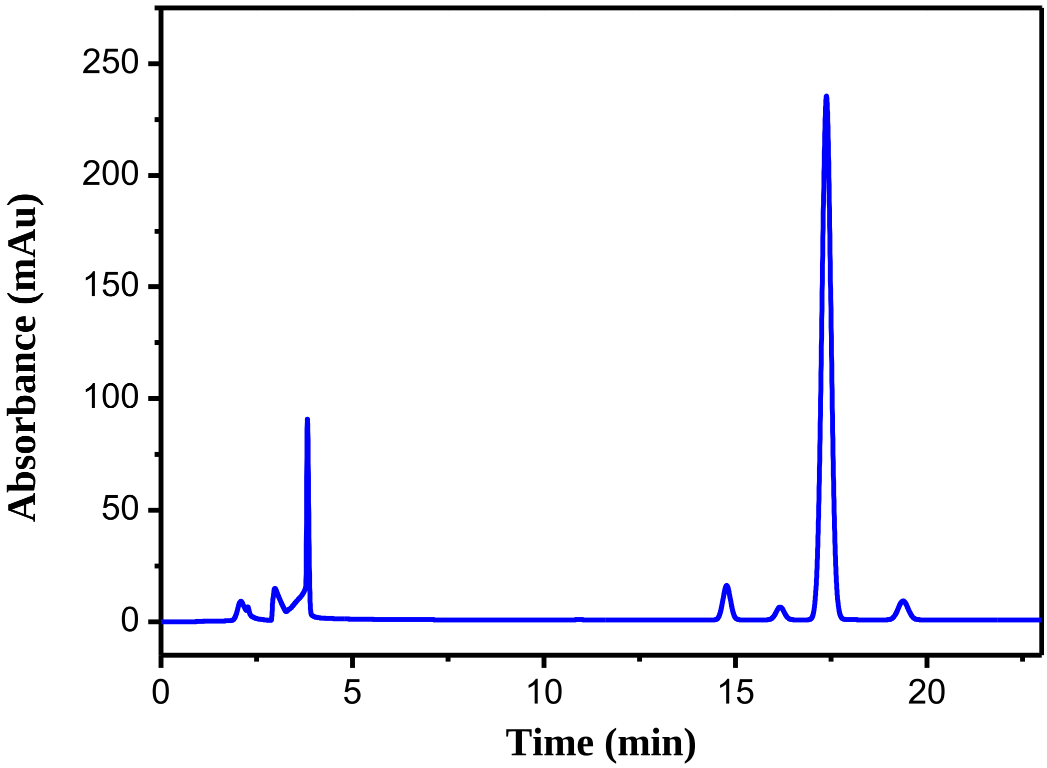

Figure S12. HPLC chromatograms of the photo-production of *c,t*-HDA (RT=14.77 min), *c,c*-HDA (RT=16.17 min), *t,t*-HDA (RT=17.37 min), and *t,c*-HDA (RT=19.38 min) on irradiation of 100 µM *t,t*-HDA for 40 min at pH = 5.0 in 10 mg C/L SRNOM.

[Sorbate]$_0$=100 μM

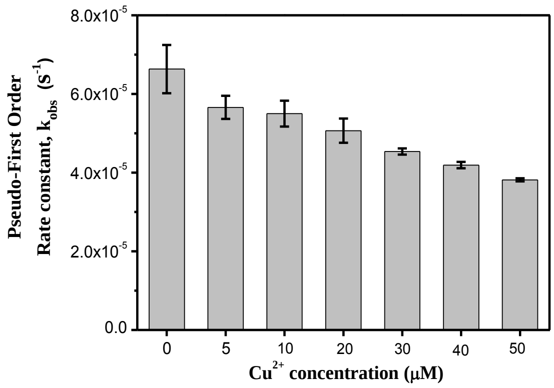

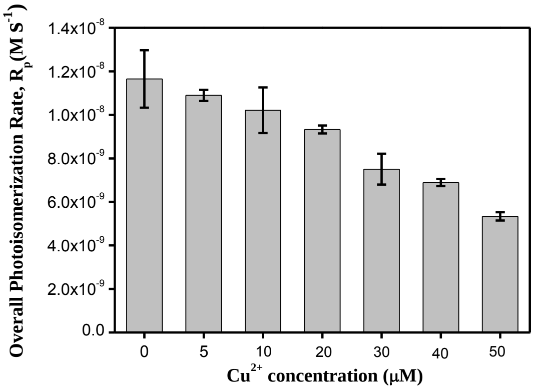

[Sorbate]$_0$=250 μM

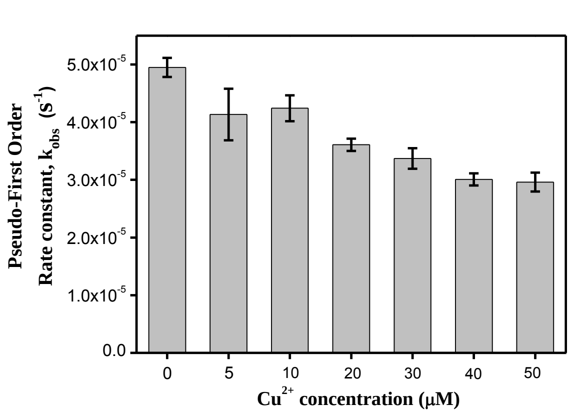

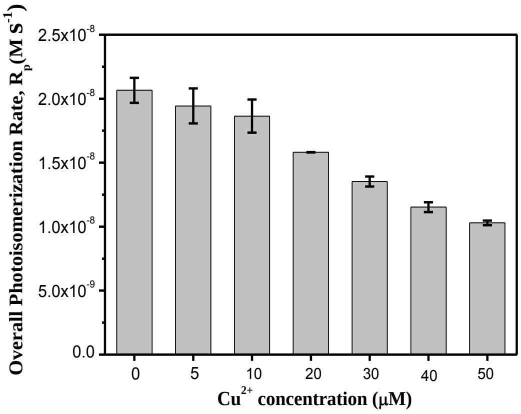

[Sorbate]$_0$=500 μM

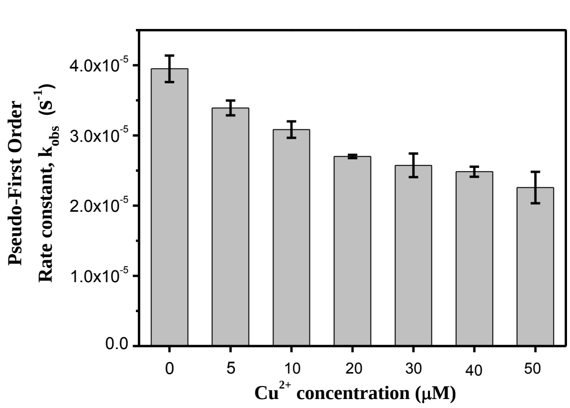

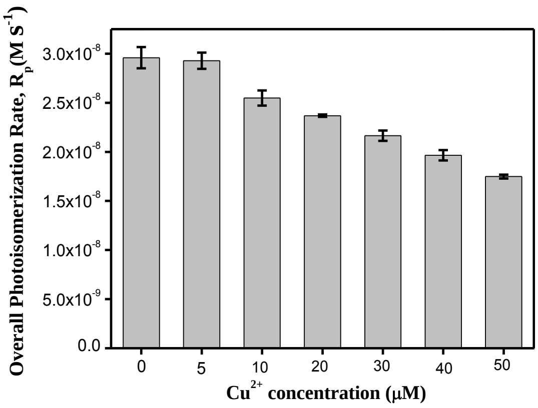

$[Sorbate]_0$=750 μM

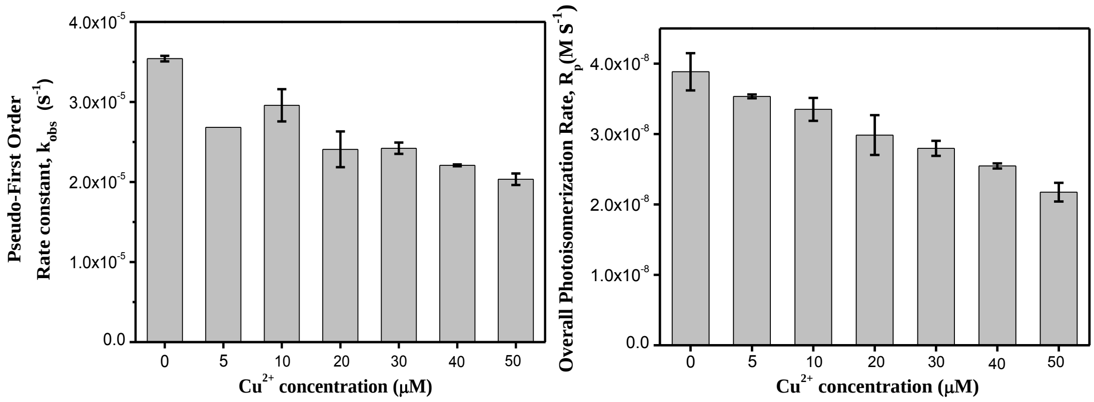

$[Sorbate]_0$=1000 μM

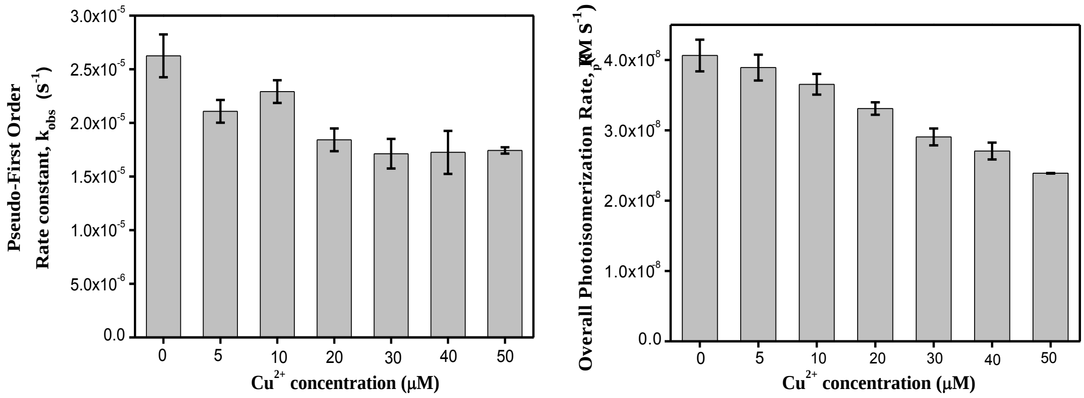

Figure S13. Pseudo-first order rate constant and overall photoisomerization rate of sorbic acid (100−1000 μM) in the absence and presence of Cu(II) upon irradiation by simulated sunlight. Conditions: SRNOM = 10 mg C/L, pH =5.0, DO (dissolved oxygen) = 226 μM.

Table S1. Measured formation rates, loss rate constants and steady-state concentrations of high energy ^{3}NOM* in the absence and presence of Cu(II). Conditions: SRNOM=10 mg C/L, pH =5.0

Cu(II) dose (μM)	F_T (10^{-8} M.s^{-1})	k' (10^5 s^{-1})	[^{3}NOM*]$_{ss}$ (10^{-13} M)	R^2
0	5.95±0.02	2.91±0.23	2.05±0.15	0.982
5	5.84±0.11	3.10±0.10	1.89±0.03	0.989
10	5.45±0.10	3.13±0.35	1.76±0.19	0.980
20	4.79±0.15	3.05±0.15	1.57±0.03	0.970
30	4.42±0.27	3.95±0.05	1.12±0.08	0.991
40	4.71±0.18	4.43±0.07	1.06±0.02	0.974
50	3.69±0.06	4.20±0.26	0.88±0.07	0.973

Text S2. Quantification of the quenching rate constant of ^{3}SRNOM* by Cu

The formation rate of singlet oxygen ($^1O_2$) in the absence of Cu(II), $R_{^1O_2}$, is obtained using the following equation:

$$R_{^1O_2} = R_{triplet} \frac{k_{O_2}[O_2]}{k_d + k_{O_2}[O_2]} \qquad (S8)$$

where $R_{triplet}$ is the formation rate of ^{3}NOM*, k_{O_2} is the quenching rate constant for ^{3}NOM* by O_2, and k_d represents the physical quenching for ^{3}NOM* by all other entities except O_2. Meanwhile, based on the FFA probe method, $R_{^1O_2}$ also can be calculated as:

$$R_{^1O_2} = (k_s + k_{^1O_2,FFA}[FFA])[^1O_2]_{ss} \qquad (S9)$$

where k_s represents the relaxation rate constant of $^1O_2$ in water.

The formation rate of ^{3}NOM* that can produce $^1O_2$, is assumed not to be affected by the presence of Cu(II) due to its much lower triplet energy required than that can sensitized isomerization of sorbate. Thus, the formation rate of $^1O_2$ in the presence of Cu, $(R_{^1O_2})_{Cu}$ can be written as:

$$(R_{^1O_2})_{Cu} = R_{triplet} \frac{k_{O_2}[O_2]}{k_d + k_{O_2}[O_2] + k_{Cu}[Cu]_{tot}} \qquad (S10)$$

$$(R_{^1O_2})_{Cu} = (k_s + k_{^1O_2,FFA}[FFA])[^1O_2]_{ss\ Cu} \qquad (S11)$$

where k_{Cu} is the quenching rate constant for ^{3}NOM* by Cu, and $[^1O_2]_{ss\ Cu}$ is the steady-state concentration of $^1O_2$ in the presence of Cu. Thus, combined with Eq 9 and 11 :

$$\frac{[^1O_2]_{ss\ Cu}}{[^1O_2]_{ss}} = \frac{(R_{^1O_2})_{Cu}}{R_{^1O_2}} = \frac{k_d + k_{O_2}[O_2]}{k_d + k_{O_2}[O_2] + k_{Cu}[Cu]_{tot}} \qquad (S12)$$

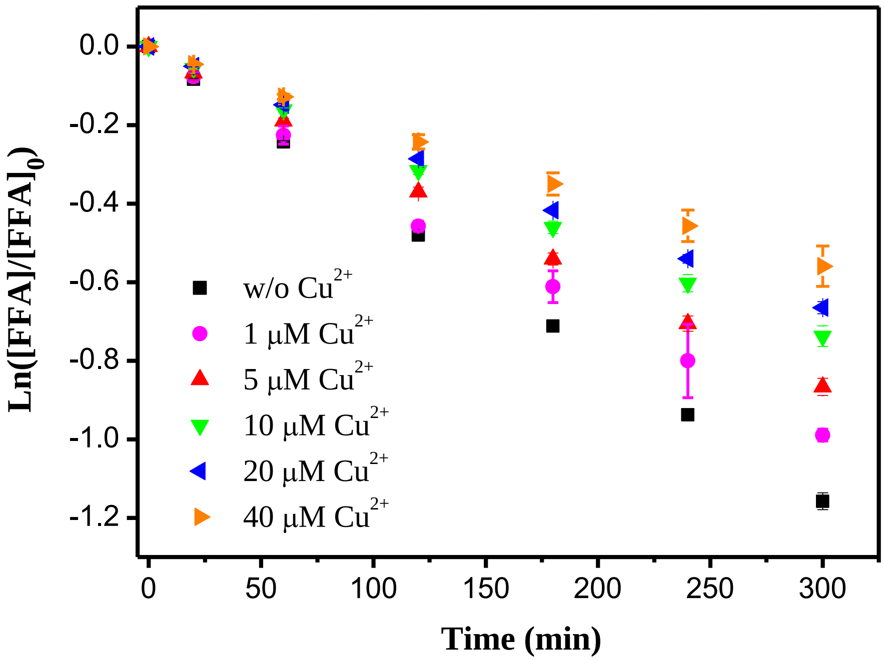

Figure S14. Photodegradation of FFA (30 μM) in the absence and presence of Cu(II) under simulated sunlight. Conditions: SRNOM = 10 mg C/L, pH = 5.0, DO (dissolved oxygen) = 226 μM.

Table S2. Steady-state concentrations of singlet oxygen in the absence and presence of micomolar Cu(II) under simulated sunlight. Conditions: SRNOM=10 mg C/L, pH =5.0

Cu(II) dose (μM)	$[^1O_2]_{ss}$ (10^{-13} M)	R^2
0	5.56 ± 0.09	0.999
1	4.77 ± 0.30	0.992
5	4.19 ± 0.11	0.998
10	3.57 ± 0.13	0.998
20	3.22 ± 0.06	0.998
40	2.72 ± 0.23	0.996

Text S3. Details of the kinetic model

Based on the analysis presented in the manuscript, the main features of the kinetic model (see Table 1 in the main paper) are discussed in detail below.

S3.1 Generation of triplet NOM and instantaneous establishment of steady-state singlet oxygen concentration

Reaction 1 represents the formation of ^{3}NOM* on absorption of photon by SRNOM. The rate constant for reaction 1 is determined by the measured H_2O_2 generation rates and TMP photooxidation rates in irradiated SRNOM solution based on a bulk carbon concentration of 40.83 mmol.g^{-1} SRNOM as reported earlier. [6] ^{3}NOM* is quenched by oxygen resulting in the formation of $^1O_2$ (reaction 2). The $^1O_2$ formed in reaction 2 reaches a steady-state almost instantaneously due to its rapid relaxation of the excited singlet state in solution (Reaction 3). The rate constant for quenching of ^{3}NOM* by oxygen was assumed to be 1.0×10^9 M^{-1} s^{-1} from Mcneill's latest results.[7] A value of 2.4×10^5 s^{-1} was used as the rate constant for the relaxation reaction (Reaction 3), assuming that relaxation of $^1O_2$ mainly occurs via its interaction with water.[8]

S3.2 Superoxide formation during irradiation

Superoxide formation during irradiation was modeled using Reactions 4 and 5. Reaction 4 shows formation of O_2-reducing radical ($Q^{\bullet-}$) on photoexcitation of Q. Reaction 4 is an apparent reaction incorporating excitation of Q, relaxation of the excited molecule back to ground state, and reduction of the excited state by electron donor. The rate of $Q^{\bullet-}$ formation is expected to be limited by the photoexcitation step because intramolecular electron transfer typically occurs very rapidly (often above the diffusion controlled limit). The apparent rate constant for reduction of Q to $Q^{\bullet-}$ was determined based on best-fit to the measured H_2O_2 concentration in irradiated SRNOM solution (Figure S7), assuming that the initial concentration of Q is the same as the concentration of electron accepting moieties in SRNOM as reported earlier.[9] It was assumed that the reaction of $Q^{\bullet-}$ with O_2 (Reaction 5) occurs at a diffusion controlled rate (i.e. with a rate constant of ~1×10^9 $M^{-1}s^{-1}$).

S3.3 Uncatalyzed disproportionation of superoxide

As described in reaction 6 (Table 1), H_2O_2 is formed as a result of uncatalyzed disproportionation of superoxide with the rate constant reported earlier by Bielski and coworkers.[10]

S3.4 Oxidative superoxide sink

Superoxide also decays due to interaction with organic radical generated on irradiation of SRNOM (see reactions 7-9 in Table 1). The rate constant for reactions 8 and 9 used here are the same as that reported in our previous study.[11] Since, the rate constant for generation of organic radicals varies with the light intensity, the value used here is different than the value reported in our earlier work[11] due to difference in the light source used; however we have assumed that the ratio of superoxide generation rate and organic radical generation rate used here is the same as that reported in our earlier work.[11]

S3.5 LMCT mediated Cu(II) reduction

Reactions 10 represent the LMCT-mediated reduction of SRNOM complexed

Cu(II) occurring under irradiated conditions. The rate constants for this reaction was obtained based on the best-fit to the measured steady-state Cu(I) concentration (Figure 2 in the main paper).

S3.6 Superoxide mediated Cu(II) reduction and Cu(I) oxidation

Superoxide-mediated Cu(II) reduction is reported to occur in earlier studies.[12, 13] However, this reaction was not important under the experimental conditions investigated here since addition of superoxide dismutase (an enzyme which catalyses the decay of superoxide) increased Cu(I) formation in irradiated SRNOM solution containing Cu(II) (Figure S14). This observation further supports that superoxide acts as Cu(I) oxidant rather than Cu(II) reductant. The rate constant for superoxide-mediated Cu(II) reduction (reaction 11, Table 1) and the rate constant for superoxide-mediated Cu(I) oxidation (reaction 12, Table 1) was determined based on best-fit to measured impact of SOD addition on Cu(I) formation.

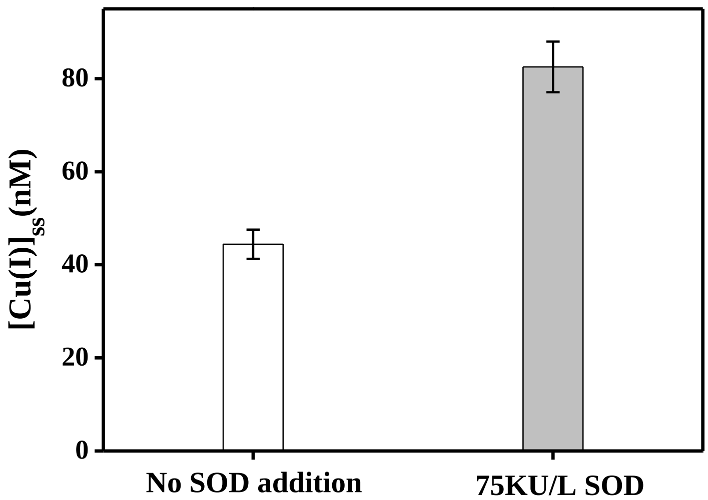

Figure S15. Effect of SOD addition on the steady-state concentrations of Cu(I) generated under irradiation of Cu(II) in 10 mgC/L SRNOM solution. Conditions: initial Cu(II) concentration = 400 nM, pH = 5.0, DO (dissolved oxygen) = 226 μM.

S3.7 Cu(I) oxidation by oxygen

Reaction 13 represents oxidation of Cu(I) by oxygen. The rate constant for this reaction is determined based on the best fit to measured Cu(I) oxidation rate in deoxygenated SRNOM solution in dark. (Figure S15).

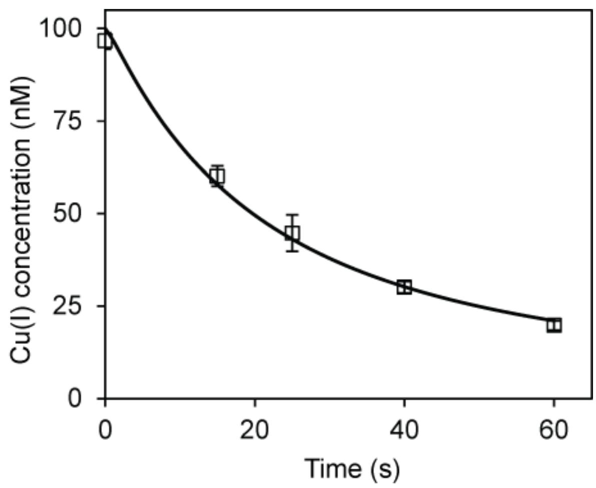

Figure S16. Cu(I) oxidation in non-irradiated 10 mgC/L SRNOM solution under deoxygenated condition. Conditions: initial Cu(I) concentration = 100 nM, pH = 5.0, DO (dissolved oxygen)= 7.5 μM.

*S3.8 Oxidation of TMP by ^{3}NOM**

Reactions 14 and 15 represent the ^{3}NOM* oxidation of TMP with the rate constant for these reactions determined based on best-fit to the measured TMP degradation rates (Figure 1) and the impact of TMP addition on H_2O_2 generation rates in irradiated SRNOM solution (Figure S7).

S3.9 Reformation of TMP by Cu(I)- TMP$^{\bullet}_{(-H)}$ interaction

As discussed in the main manuscript, Cu decreases the photooxidation rate of TMP due to the interaction of the radical intermediate ($TMP^{\bullet}_{(-H)}$) with photo-generated Cu(I) (Reaction 16). The rate constant for this reaction is determined based on the best-fit to the measured TMP oxidation rates (Figure 1).

S3.10 Additional H_2O_2 source in the presence of TMP

As discussed in the main paper, the generation rate of H_2O_2 increases in irradiated SRNOM solution with TMP addition. This is due to the increased generation of oxygen reducing radicals by TMP addition.[14] To simplify the model, we have assumed that these oxygen reducing radicals are different from that generated in the absence of TMP. We have further assumed that the reduced NOM radical, formed by the interaction of TMP with $^3NOM^*$ (reaction 14), is responsible for H_2O_2 generation via oxygen reduction (reaction 17). The rate constant for reaction 17 is assumed to be diffusion-limited. Reaction 18 represents relaxation of NOM^- to form a non-reactive product (NRP) with the rate constant for this reaction determined based on the best-fit to measured H_2O_2 concentration in the presence of TMP (Figure S7).

REFERENCES

1. Grebel, J. E.; Pignatello, J. J.; Mitch, W. A., Sorbic acid as a quantitative probe for the formation, scavenging and steady-state concentrations of the triplet-excited state of organic compounds. *Water Res.* **2011,** *45* (19), 6535−6544.
2. Zeng, T.; Arnold, W. A., Pesticide photolysis in prairie potholes: probing photosensitized processes. *Environ. Sci. Technol.* **2012,** *47* (13), 6735−6745.
3. Chen, C. Y.; Zepp, R. G., Probing Photosensitization by Functionalized Carbon Nanotubes. *Environ. Sci. Technol.* **2015,** *49* (23), 13835−13843.
4. Zepp, R. G.; Schlotzhauer, P. F.; Sink, R. M., Photosensitized transformations involving electronic energy transfer in natural waters: role of humic substances. *Environ. Sci. Technol.* **1985,** *19* (1), 74−81.
5. Halladja, S.; Ter Halle, A.; Aguer, J.-P.; Boulkamh, A.; Richard, C., Inhibition of humic substances mediated photooxygenation of furfuryl alcohol by 2, 4, 6-trimethylphenol. Evidence for reactivity of the phenol with humic triplet excited states. *Environ. Sci. Technol.* **2007,** *41* (17), 6066−6073.
6. Aeschbacher, M.; Graf, C.; Schwarzenbach, R. P.; Sander, M., Antioxidant

Properties of Humic Substances. *Environ. Sci. Technol.* **2012,** *46*(9), 4916−4925.
7. McNeill, K., Using direct observation of singlet oxygen to determine triplet organic matter rate constants. *253^th^* ACS National Meeting, San Francisco, CA.April 2−6, **2017**.
8. Wilkinson, F.; Helman, W. P.; Ross, A. B., Rate Constants for the Decay and Reactions of the Lowest Electronically Excited Singlet State of Molecular Oxygen in Solution. An Expanded and Revised Compilation. *J. Phys. Chem. Ref. Data.* **1995.** *24(2)*, 663−677.
9. Aeschbacher, M.; Sander, M.; Schwarzenbach, R. P., Novel electrochemical approach to assess the redox properties of humic substances. *Environ. Sci. Technol.* **2010,** *44*, 87−93.
10. Bielski, B.; Cabelli, D.; Arudi, R.; Ross, A., Reactivity of $HO_2/O_2^{\bullet -}$ Radicals in Aqueous Solution. *J. Phys. Chem. Ref. Data.* **1985,** *14*, 1041−1100.
11. Garg, S.; Jiang, C.; Waite, T. D., Mechanistic insights into iron redox transformations in the presence of natural organic matter: Impact of pH and light. *Geochim. Cosmochim. Acta.* **2015,** *165*, 14−34.
12. Pham, A. N.; Rose, A. L.; Waite, T. D., Kinetics of Cu(II) Reduction by Natural Organic Matter. *J. Phys. Chem. A.* **2012,** *116*(25), 6590−6599.
13. Yuan, X.; Pham, A. N.; Miller, C. J.; Waite, T. D., Copper-catalyzed hydroquinone oxidation and associated redox cycling of copper under conditions typical of natural saline waters. *Environ. Sci. Technol.* **2013,** *47* (15), 8355−8364.
14. Zhang, Y.; Simon, K. A.; Andrew, A. A.; Del, V. R.; Blough, N. V., Enhanced photoproduction of hydrogen peroxide by humic substances in the presence of phenol electron donors. *Environ. Sci. Technol.* **2014,** *48* (21), 12679−12688.